Electronic Supplementary Material (ESI) for Physical Chemistry Chemical Physics.

Molecular Dynamics Investigation of Benzoic Acid in Confined Spaces

Luca Sironi[1], Giovanni Macetti[1], Leonardo Lo Presti*[,1,2]

1. Università degli Studi di Milano, Department of Chemistry, Via Golgi 19, 20133 Milano (Italy)

2. Istituto Nazionale di Fisica Nucleare (INFN), Laboratori Nazionali di Frascati, Frascati (Italy)

* To whom correspondence should be addressed: leonardo.lopresti@unimi.it

SUPPORTING INFORMATION

Table of contents

S1. Full description of the confinement algorithm

S1.1. Algorithm

To perform a confined molecular dynamics simulation, MiCMoS needs (i) a pre-equilibrated simulation box and (ii) a topology file as input. These can be obtained with standard MiCMoS procedures, which include for example routines like *boxliq* and *pretop* (see the MiCMoS manual for full details).[1] The routine *boxliq* reads an *.oeh* structure file and creates an ensemble of randomly oriented molecules (extension *.dat*), which needs to be pre-equilibrated with Monte Carlo to dispose of hard contacts and adjust the starting density. The topology can be created from the same *.oeh* file with *pretop* and edited at user's convenience to set up the correct potential for torsional parameters.

The starting liquid is given in input to a new module, *confbox* (Section 1.2 SI). This program is used to prepare the parameter file *barrier.par*, which specifies the geometrical details of the confined space and the force field parameters of the barrier (Section 1.3 SI). At the same time, *confbox* converts the standard simulation box for the unconfined liquid into a new simulation box named **confined.dat*, which is ready for the confined simulation. Essentially, *confbox* deletes all the molecules which bear an atom in close contact (less than the sum of the van der Waals radii) with the barrier.

A new parameter, `inano`, must be specified in the input *.mdi* file. This is read as an integer in 7th position, command line 2. `inano` = 0 means unconfined simulations and implies that the *confbox* procedure described above is not needed, while `inano` = 1, 2, 3 may be set for nanolayer, nanotube, and nanocavity simulations respectively.

When the MD simulation is launched, inano > 1 implies that confinement is applied on the starting simulation box by reducing the corresponding number of periodic directions. The barriers consist of regular square/rectangular grids of massless neutral pixels (see main text), whose number is calculated by rounding down the ratio between the equilibrium box size according to the maximum theoretical packing efficiency[2] and the pixel diameter. Pixels are placed tangentially to the desired faces of the simulation box, that is, the barrier is always parallel to the box surfaces.

By default, the barriers are added onto the surfaces that correspond to nonperiodic directions of the original simulation box. An offset parameter can be controlled while using *confbox*, to tune the distance between the barriers and the box boundaries. In other words, the offset parameter allows to perform a fine adjustment of the barrier position with respect to the simulation box surface. Actually, *confbox* deletes those molecules that have at least 1 atom below the van der Waals distance with at least 1 pixel of the barrier (see above). This step is mandatory to prevent steric clashes at the beginning of the simulation. Thus, the offset parameter is useful to avoid the deletion of many molecules.

If desired, the user can also choose to start with less dense liquids by acting on the parameters `nmolzacu` and `nmolzacv` specified in the *barrier.par* file (see Section S1.3 SI below). For

instance, to make a simulation with the same box dimensions but with a lower packing efficiency, it is enough to reduce the number of molecules in the simulation box, keeping constant `nmolzacu`. Alternatively, it is also possible to have a lower packing efficiency also incrementing `nmolzacu` and keeping constant the number of molecules in the simulation box. In this latter case the box dimensions will be larger.

Every time the barostat varies the dimensions of the simulation box, the pixel positions are modified accordingly, but their number remains constant. Normally, during a standard, unconfined simulation, the scaling factors of box dimensions are proportional to the difference between the reference pressure of the barostat and the pressure calculated from the virial of the forces. If the pressure of the system is high and positive in a specific direction, the box dimension in that direction would increase and vice versa. To avoid unphysical stretching of the barriers, the following solution is employed. A fictitious pressure is added in each laboratory direction x, y, and z. This counterpressure is proportional to the difference between the actual box size and the equilibrium box size, divided by the area of the face orthogonal to that direction. The proportionality constant k is the one of a Csp^2-Csp^2 bond (3400 $kJ \cdot mol^{-1} \cdot Å^{-2}$). A damping scale factor is also applied by the user, as specified in the barrier.par parameter file. At the very beginning of the simulation, in particular if a large offset is set between the faces of the simulation box and the barriers, this procedure would give a high negative pressure, that might compress the system producing clashes between atoms in close contact. For this reason, when the confinement is active (`inano` > 0), a further damping is automatically applied to the barostat algorithm. In particular, the barostat is prevented from applying (an)isotropic scaling factors lower than 0.95 to the box edge lengths or, equivalently, changes not larger than 5 % are allowed for the box edge lengths in a single MD step.

S1.2 Confbox routine

The program reads a file with extension *.dat* that contains an equilibrated liquid and prompts the following parameters from the keyboard:

1) inano — type of confinement
   - =0 none
   - =1 nanolayer
   - =2 nanotube
   - =3 nanocavity
2) iplane — active confining planes (XY, XZ, YZ), not required if inano=3
3) thickness — distances between the barriers in Å for each couple of confining planes
   - =0 default, a whole box edge
4) rvdw,ispbar,offset
   - rvdw — radius of the pixels
   - ispbar — atom type to describe the C_6 and C_{12} Lennard Jones parameters of the pixels that make up the barrier. This corresponds to the atom id code specified in Table 1.1 in the MiCMoS user's manual.
   - offset — offset distance (in Å) between the barrier and the starting simulation box edge to avoid the deletion of a large number of protruding molecules (see Section S1.1 SI for more information)
5) iattr — determines whether to use the attractive part of the potential for the description of the barriers
   - =0 repulsive-only potential
   - =1 full van der Waals potential
6) dampk — 3 scaling factors applied to the force constants along z, y, and x direction, used to tune the stiffness of the barrier
7) zacsize, nmolzacu, nmolzacv
   - zacsize — equilibrium distance between the barriers of the nanolayer or the squared nanotube (optional, 0=default which is a cubic simulation box)
   - nmolzacu — number of molecules to consider for the determination of the equilibrium volume of the simulation box, used to have a different packing efficiency with respect to 0.66, according to Zaccone (0=default which is the number of solute molecules). See Section S1.1 SI for some examples.
   - nmolzacv — the same of nmolzacu but for the solvent molecules

S1.3 Parameter file

1) #comment line
2) iplane(XY), iplane(XZ), iplane(YZ), iattr
   - iplane: 3 values that set the confining planes to use (plane XY, XZ, YZ)
     - =0 inactive
     - =1 active
   - iattr: Determines whether to use the attractive part of the potential for the description of the barriers
     - =0 repulsive-only potential
     - =1 full van der Waals potential
3) #comment line
4) ispbar, rvdw, qqbar, offset
   - ispbar: atom type to describe the C_6 and C_{12} Lennard Jones parameters of the pixels that make up the barrier
   - rvdw: radius of the pixels
   - qqbar: charge of the pixels
   - offset: offset distance (in Å) between the barrier and the starting simulation box to avoid the deletion of a large number of protruding molecules
5) #comment line
6) dampk(XY), dampk(XZ), dampk(YZ)
   - dampk: 3 scaling factors applied to the force constants along z, y, and x direction, used to tune the stiffness of the barrier
7) #comment line
8) zacsize, nmolzacu, nmolzacv
   - zacsize: equilibrium distance between the barriers of the nanolayer or the squared nanotube (optional, 0=default which is a cubic simulation box)
   - nmolzacu: number of molecules to consider for the determination of the equilibrium volume of the simulation box, used to have a different packing efficiency with respect to 0.66, according to the theoretical limit of maximum packing efficiency (0=default which is the number of solute molecules). See Section S1.1 SI for some examples.
   - nmolzacv: the same of nmolzacu but for the solvent molecules.

S2. Molecular geometry and MiCMoS input files

S2.1. Input MD .mdi file

```
Benzoic acid ljc 350 K liq unbiased nanolayer
# n.steps irvel ipri ibox idstr timestep Emolim iengt ibias + Ebias Nbias
  500000     0      0      1    1     0.001   -5.0    0     0
# cutoffu cutoffv cutoffuv factin  ipots ianh inano
   16.0    0.0     0.0       0.7      1    0    1
#  N(T)   Tset Tstart Trelax  0/1 weak/stiff
    100    350   350    0.6      0
#  N(P) Pset comprs 0/1ianis ipr ww  iextstr+stra11 22,33,12,13,23,GPa
     50    1.0   0.4      1      0    0.0    0
#  N(com)  nwbox   nwre  npri
    100     500    500    500
```

S2.2. Input barrier.par file

```
# iplane(XY), iplane(XZ), iplane(YZ), iattr
         1         0         0         0
# ispbar,    rvdw,    qqbar,    offset
    12    1.7700      0.000000    6.0000
# dampk(XY),  dampk(XZ),  dampk(YZ)
  0.025000  0.025000  0.025000
# zacsize,      nmolzacu,   nmolzacv(0=default)
    0.000000         0         0
```

S2.3. Topology .top file

```
#BENZAC02 'P 21/c'   topology  MD LJC
   15
    1  -0.00013  -0.00497   0.17693  12    0.1028
    2   0.00727   1.20076  -0.50719  12   -0.1934
    3   0.00790   1.19827  -1.89054  12   -0.0681
    4  -0.00200   0.02343  -2.58619  12   -0.1361
    5  -0.00762  -1.17770  -1.90681  12   -0.0449
    6  -0.00426  -1.19365  -0.52904  12   -0.2206
    7   0.01252   2.13453   0.03549   2    0.1289
    8   0.01632   2.13602  -2.42626   2    0.1074
    9  -0.00540   0.03424  -3.66606   2    0.1134
   10  -0.01472  -2.10748  -2.45637   2    0.1055
   11  -0.00491  -2.13536  -0.00030   2    0.1482
   12  -0.00116  -0.02685   1.66112  10    0.6016
   13  -0.01301   1.06740   2.28285  27   -0.5857
   14   0.01367  -1.15566   2.23684  27   -0.5303
   15  -0.01433   1.10913   3.28194   6    0.4714
    0  nslav-u
    0  ncore-v
    0  nslav-v
  112.0    0.0 volu-u,volu-v
   15  nstr-u
    1    2   1.386  4958.6   C- C
    1    6   1.383  5038.1   C- C
    1   12   1.484  2894.0   C- C
    2    3   1.383  5020.8   C- C
    2    7   1.080  3600.0   C- H
    3    4   1.365  5399.2   C- C
    3    8   1.080  3600.0   C- H
```

```
  4    5   1.380  5091.9   C- C
  4    9   1.080  3600.0   C- H
  5    6   1.378  5136.3   C- C
  5   10   1.080  3600.0   C- H
  6   11   1.080  3600.0   C- H
 12   13   1.259  7254.9   C- O
 12   14   1.267  7061.6   C- O
 13   15   1.000  4250.0   O- H
  0  nstr-v
 22  nbend-u
  1    2    3  119.00   576.7   C- C- C
  1    2    7  120.00   505.0   C- C- H
  1    6    5  120.00   583.8   C- C- C
  1    6   11  120.00   505.0   C- C- H
  1   12   13  119.00   655.6   C- C- O
  1   12   14  118.00   637.5   C- C- O
  2    1    6  120.00   583.8   C- C- C
  2    1   12  120.00   583.8   C- C- C
  2    3    4  121.00   590.8   C- C- C
  2    3    8  120.00   505.0   C- C- H
  3    2    7  120.00   505.0   C- C- H
  3    4    5  120.00   583.8   C- C- C
  3    4    9  120.00   505.0   C- C- H
  4    3    8  120.00   505.0   C- C- H
  4    5    6  120.00   583.8   C- C- C
  4    5   10  120.00   505.0   C- C- H
  5    4    9  120.00   505.0   C- C- H
  5    6   11  120.00   505.0   C- C- H
  6    1   12  120.00   583.8   C- C- C
  6    5   10  120.00   505.0   C- C- H
 12   13   15  122.00   450.0   C- O- H
 13   12   14  123.00   727.7   O- C- O
  0  nbend-v
 15  ntors-u
 6   1   2   3  50.00   -1.0    1.0   C- C- C- C
 2   1   6   5  50.00   -1.0    1.0   C- C- C- C
 2   1  12  13  14.00   -1.0    2.0   C- C- C- O
 1   2   6  12 100.00   -1.0    1.0   C- C- C- C
 1   2   3   4  50.00   -1.0    1.0   C- C- C- C
 2   1   3   7 100.00   -1.0    1.0   C- C- C- H
 2   3   4   5  50.00   -1.0    1.0   C- C- C- C
 3   2   4   8 100.00   -1.0    1.0   C- C- C- H
 3   4   5   6  50.00   -1.0    1.0   C- C- C- C
 4   3   5   9 100.00   -1.0    1.0   C- C- C- H
 4   5   6   1  50.00   -1.0    1.0   C- C- C- C
 5   4   6  10 100.00   -1.0    1.0   C- C- C- H
 6   1   5  11 100.00   -1.0    1.0   C- C- C- H
 1  12  13  15  35.00   -1.0    2.0   C- C- O- H
12   1  13  14 100.00   -1.0    1.0   C- C- O- O
  0  ntors-v
  2  nlist-u
7 15 11 15
  0  nlist-v
 0.410   235.0   650.0   77000.0
  0  nextr
```

S3. Gromacs simulation of the bulk liquid phase

S3.1. Simulation details

The benzoic acid molecule was parametrized following the same procedure described elsewhere,[3] which is fully automatized on the Automatic Topology Builder webserver (https://atb.uq.edu.au/index.py).[4] The topology file (ATB molid: 1208959, ATB Topology Hash: 95724) was used in conjunction with the same simulation box (432 molecules) equilibrated by MiCMoS for 500 ps (see the main text). Molecular dynamics simulations were carried out with Gromacs[5] v2018.4 using the gromos54a7 force field. Pre-production equilibration was carried out for 100 ps in NVT and NpT (1 bar, T = 350 K) conditions under isotropic pressure coupling. Then, a 1 ns-long NpT molecular dynamics run was performed, allowing a time step of 2 fs with the leap-frog integrator. An isotropic Berendsen barostat[6] was used to restrain the pressure to 1 bar, while temperature was regulated at 350 K with the stochastic CSVR algorithm.[7] All the covalent bonds were constrained to their equilibrium lengths through the LINCS algorithm,[8] while the Particle Mesh Ewald (PME) method[9] was used to treat long-range electrostatics in conjunction with a 10 Å cutoff for non-bonded interactions. The parameters of the simulation were chosen to be as similar as possible to the MiCMoS one.

S3.2. Comparison with MiCMoS simulation

Figure S1 compares the rotational correlation functions, as predicted by MiCMoS and Gromacs. The agreement is qualitative. As regards Gromacs simulations, the main inertial axis $\mathbf{v}_1$ (C1–C4 vector, inset) slowly loses its rotational correlation in both simulations, as 200 ps are needed to appreciate a 80% reduction of $C(t)$. On the contrary, rotations around the axis perpendicular to the aromatic ring are much easier, with a 80% large loss of correlation appreciable in ~60 ps, that is, out-of-plane rotations of the phenyl ring are roughly three times faster. This is clearly a shape effect: easy librations around the main molecular axis do not imply a change in the orientation of the axis itself. MiCMoS results are qualitatively similar, with generally slower rotational motions and out-of-plane rotations of the phenyl being ~2.3 times faster than rotations of the main inertial axis. However, the conformity of views of MiCMoS with available data on the liquid viscosity (Table S1) reassures us on the general validity of the LJC force field.

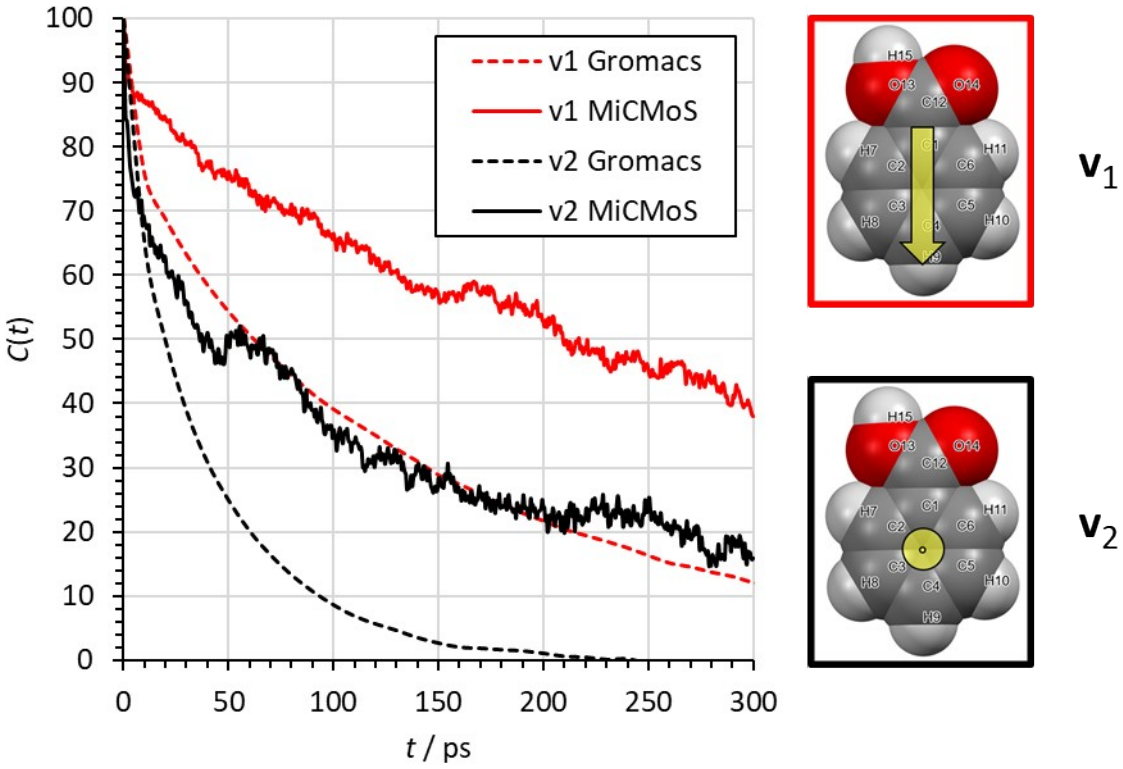

Figure S1. Comparison of Gromacs and MiCMoS estimates for the rotational correlation function of benzoic acid, $C(t)$. The reference frame (t = 0 in the plot) is 200 ps for MiCMoS and 500 ps for Gromacs simulation.

Table S1. Self-diffusion coefficients (D), dynamic shear diffusion viscosities η and densities from MD simulations of unconfined benzoic acid liquids, using MiCMoS and Gromacs. Standard deviations are reported in parentheses.

	$D \times 10^{-10}$ / $m^2 \cdot s^{-1}$	$\eta \times 10^3$ / Pa·s	ρ / $g \cdot cm^{-3}$
Bulk liquid, MiCMoS	3.27(1)	2.6(2)	1.109(8)
Bulk liquid, Gromacs[a]	3.12(6)	2.90(6)	1.156(1)

[a] gromos54a7 force field, same number of molecules in the simulation box as MiCMoS. The parameters were evaluated from the last 300 ps of the trajectory by fitting the $D(t)$ vs. m.s.d. Einstein relationship.

S4. Translational diffusion

Table S2 compares the values of self-diffusion coefficients, viscosities and densities for the confined simulations, either with full van der Waals or repulsive-only barriers, with 432 molecules and 41.874 Å reference distance between barriers. There is a general reduction of self-diffusion coefficients (and consequent increment of viscosities) increasing the number of non-periodic directions (N_{NP}), i.e. passing from nanolayers to nanocavities. This is consistent with the reduction of translational degrees of freedom that hampers the diffusion. In addition, density decreases with the increase of N_{NP}. When repulsive-only barriers are employed, diffusion is lower (viscosity is greater) compared to full van der Waals barriers, and density is lower as well.

Table S2. Self-diffusion coefficients (D), dynamic shear diffusion viscosities η and densities from MD simulations of nanoconfined benzoic acid liquids with 432 molecules. Standard deviations are reported in parentheses.

	N_{NP} [a]	Barrier	$D \times 10^{-10}$ / $m^2 \cdot s^{-1}$	$\eta \times 10^3$ / Pa·s	ρ / $g \cdot cm^{-3}$
Nanolayer	1	Full vdW	0.867(5)	9.89(6)	1.158(6)
Nanotube	2	Full vdW	0.833(8)	10.3(1)	1.145(7)
Nanocavity	3	Full vdW	0.564(5)	15.2(1)	1.139(7)
Nanolayer	1	Rep only	0.661(5)	13.0(1)	1.144(5)
Nanotube	2	Rep only	0.541(6)	15.8(2)	1.128(7)
Nanocavity	3	Rep only	0.483(6)	17.7(2)	1.112(7)

[a] Number of non-periodic dimensions

Table S3 shows the same results as regards simulations with a double number of molecules (864) and with the reference distances between barriers 50% larger for nanolayers and squared nanotubes and increased by a factor $\sqrt[3]{2}$, ~26%, for nanocavities.

Table S3. Self-diffusion coefficients (D), dynamic shear diffusion viscosities η and densities from MD simulations of nanoconfined benzoic acid liquids with 864 molecules. Standard deviations are reported in parentheses.

	N_{NP} [a]	Barrier	$D \times 10^{-10}$ / $m^2 \cdot s^{-1}$	$\eta \times 10^3$ / Pa·s	ρ / $g \cdot cm^{-3}$
Nanolayer	1	Full vdW	1.220(8)	7.03(5)	1.157(4)
Nanotube	2	Full vdW	1.074(6)	7.98(5)	1.145(4)
Nanocavity	3	Full vdW	0.819(8)	10.5(1)	1.137(5)
Nanolayer	1	Rep only	0.832(4)	10.30(6)	1.145(4)
Nanotube	2	Rep only	0.788(6)	10.88(9)	1.124(4)
Nanocavity	3	Rep only	0.487(7)	17.6(2)	1.108(4)

[a] Number of non-periodic dimensions

S5. Molecular rotations

Figure S2 shows the rotational correlation functions from 200 ps to 500 ps for the nanoconfined liquids and the unconfined one using the vectors approximately parallel to the molecular dipole direction and orthogonal to the phenyl ring as reference vectors. The loss of correlation is slower in confined liquids with respect to the unconfined bulk simulation, in particular for the parallel vectors. As bulk simulation, BZA molecules in confined simulations lose correlation more quickly for the orthogonal vector.

Table S4 shows the parameters of stretched exponential, or Kohlrausch–Williams–Watts (KWW),[10,11] function used to fit the data of rotational correlation functions, and the determination coefficient. Adimensional Kohlrausch exponents (β) and rotational correlation times (τ_c) are plotted in Figure S3 which shows the presence of a correlation using parallel vectors and the absence of correlation with orthogonal vectors.

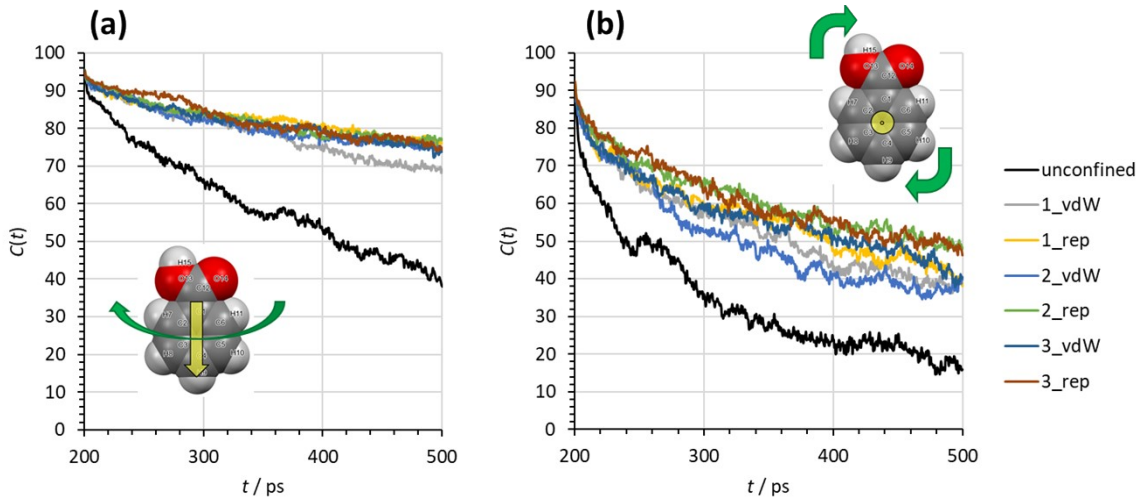

Figure S2. Rotational correlation function vs. time (ps) in confined spaces. The insets show the orientation of the corresponding reference vectors (in yellow). The labels have the following meaning: the numbers 1, 2, and 3 refers to the number of non-periodic dimensions and stand for nanolayer, nanotube, and nanocavity while vdW and rep correspond to full van der Waals and only-repulsive potential to model the barriers. Green arrows are examples of rotations that preserve the orientations of the yellow reference axis: slower relaxation times imply that molecular rotations occur preferentially in this way.

Table S4. Stretched exponential prefactor, ($C(0)$) rotational relaxation times (τ_c), Kohlrausch exponents (β) and coefficients of determination R^2 from MD simulations of nanoconfined benzoic acid liquids. Results from the bulk liquid are shown for the sake of comparison. Standard deviations are reported in parentheses.

	N_{NP}	Barrier	Axis[a]	$C(0)$	$\tau_{c/ps}$	β	R^2
Bulk liquid	0	None	⊥	89(1)	122(4)	0.56(1)	0.9784
			∥	91.0(4)	398(2)	0.829(1)	0.9905
Nanolayer	1	Full vdW	⊥	87(6)	390(4)	0.64(1)	0.9829
			∥	92.6(2)	1200(20)	0.86(1)	0.9847
Nanotube	2	Full vdW	⊥	93(1)	304(6)	0.54(1)	0.9752
			∥	97.0(4)	6300(400)	0.435(1)	0.9729
Nanocavity	3	Full vdW	⊥	88.5(8)	568(7)	0.54(1)	0.9748
			∥	97.0(6)	6300(500)	0.435(2)	0.9439
Nanolayer	1	Rep only	⊥	84.1(6)	508(5)	0.69(2)	0.9714
			∥	93.0(2)	4900(300)	0.59(2)	0.9673
Nanotube	2	Rep only	⊥	88.6(5)	724(9)	0.57(1)	0.9796
			∥	96.4(3)	6000(300)	0.48(1)	0.9769
Nanocavity	3	Rep only	⊥	91.0(6)	653(7)	0.56(1)	0.9799
			∥	95.2(3)	2600(100)	0.66(2)	0.9625

[a] Results for the axis perpendicular (⊥) and parallel (∥) to the phenyl plane are shown.

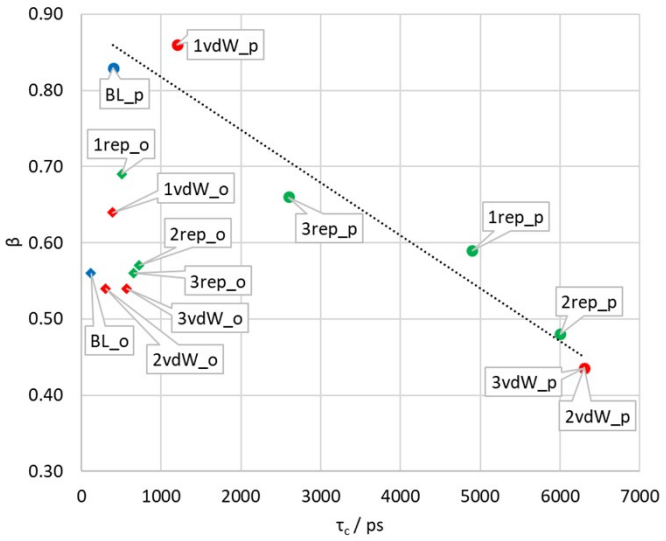

Figure S3. Adimensional Kohlrausch exponent (β) *vs*. rotational correlation time (τ_c) from simulations in confined spaces. See Table S4 for the numerical data. The labels have the following meaning: "N_{NP}-potential_axis", where "N_{NP}" is the number of non-periodic dimensions, "potential" is either "vdW" or "rep" depending on whether the barrier is modeled by full van der Waals or repulsive only potential, and "axis" is either "o" or "p" for orthogonal or parallel reference vectors with respect to the phenyl ring plane. Thus, for example, 3rep_o means nanocavity, repulsive barrier, orthogonal axis. Full van der Waals potentials are highlighted in red, repulsive-only potentials in green (dots: parallel, diamonds: orthogonal). "BL_o" and "BL_p"(blue) stand for the bulk liquid unconfined reference. The black dotted line comes from the least squares fitting against all the "parallel" vector references. The corresponding equation is $\beta = -6.9(7)\cdot10^{-5}\ \tau_c + 0.89(3)$ with $R^2 = 0.9549$. The "orthogonal" references produce no detectable correlation and are clustered at the left of the diagram.

S6. Hydrogen bonds

Benzoic acid has one HB donor and two O atoms acting as HB acceptors. In order to establish whether a hydrogen bond is present or not, we decided to use a simple distance criterion: only if the distance between the donor and the acceptor is lower than 90% of the sum of van der Waals radii (1.10 Å for H and 1.58 Å for O), that is <2.412 Å, the HB is formed. The choice of using 90% instead of 100% is conservative and was made to dispose of long intermittent contacts. These are characterized by a lifetime of less than 0.5-1 ps as exemplified in Figure S4. In general, apart from these short lifetimes, the trend is maintained. Table S5 reports the number of HBs for the different confined liquids.

Figure S5 compares the average number of HBs per frame in the different simulations. No significant differences are evident: in all cases, the average value remains the same, *i.e.* 1 HB per molecule, due to the tendency of BZA molecules to form as many hydrogen bonds as possible, regardless of the type of confinement.

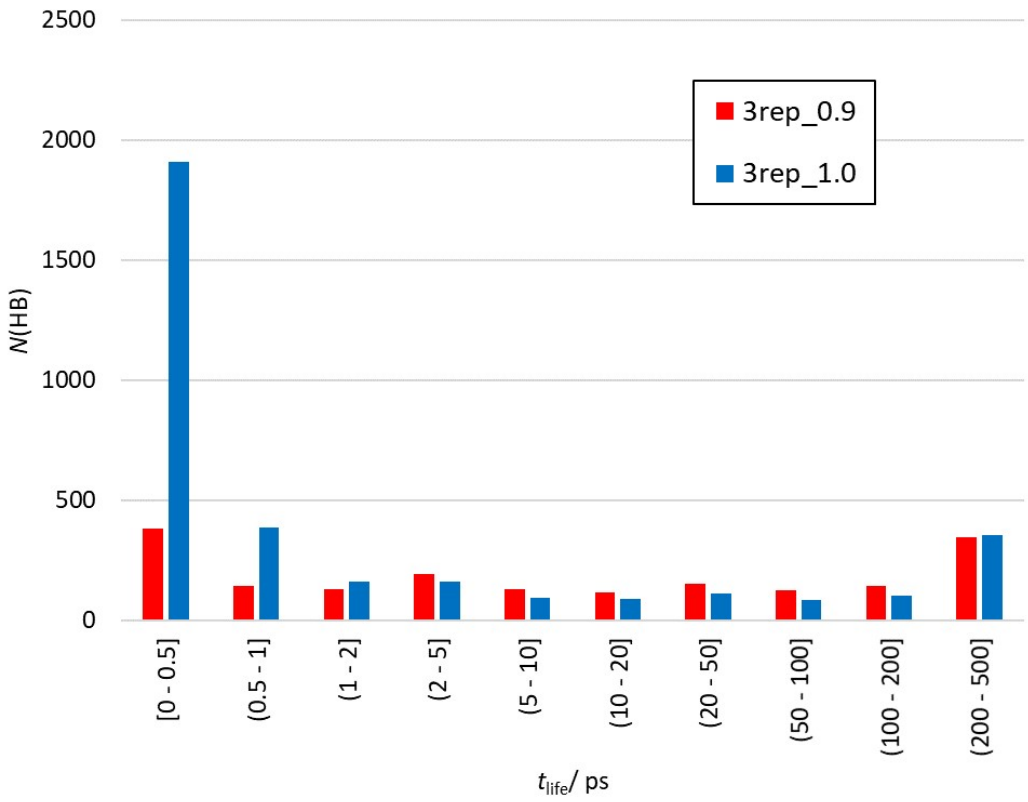

Figure S4. Number of OH···O contacts N(HB) within the threshold distance $k\times(r_{vdW,H} + r_{vdw,O})$ *vs*. the lifetime (t_{life}), k being 1.0 (blue) or 0.9 (red). Data refers to the nanocavity liquid with repulsive-only barriers.

Table S5. Number of HBs as a function of the lifetime t_life and confinement. 1, 2, 3 in the labels refer to nanolayer, nanotube and nanocavity respectively while vdW and rep stand for full van der Waals and repulsive-only potential to model the barriers.

t_life	unconfined	1_vdW	1_rep	2_vdW	2_rep	3_vdW	3_rep
(0 - 2]	296	598	557	536	625	666	655
(2 - 5]	85	155	163	133	170	186	191
(5 - 10]	62	115	122	109	126	120	131
(10 - 20]	87	118	117	101	122	117	117
(20 - 50]	114	158	136	141	160	138	152
(50 - 100]	115	120	122	118	138	96	126
(100 - 200]	167	154	138	168	181	129	141
(200 - 500]	352	343	379	364	364	365	347

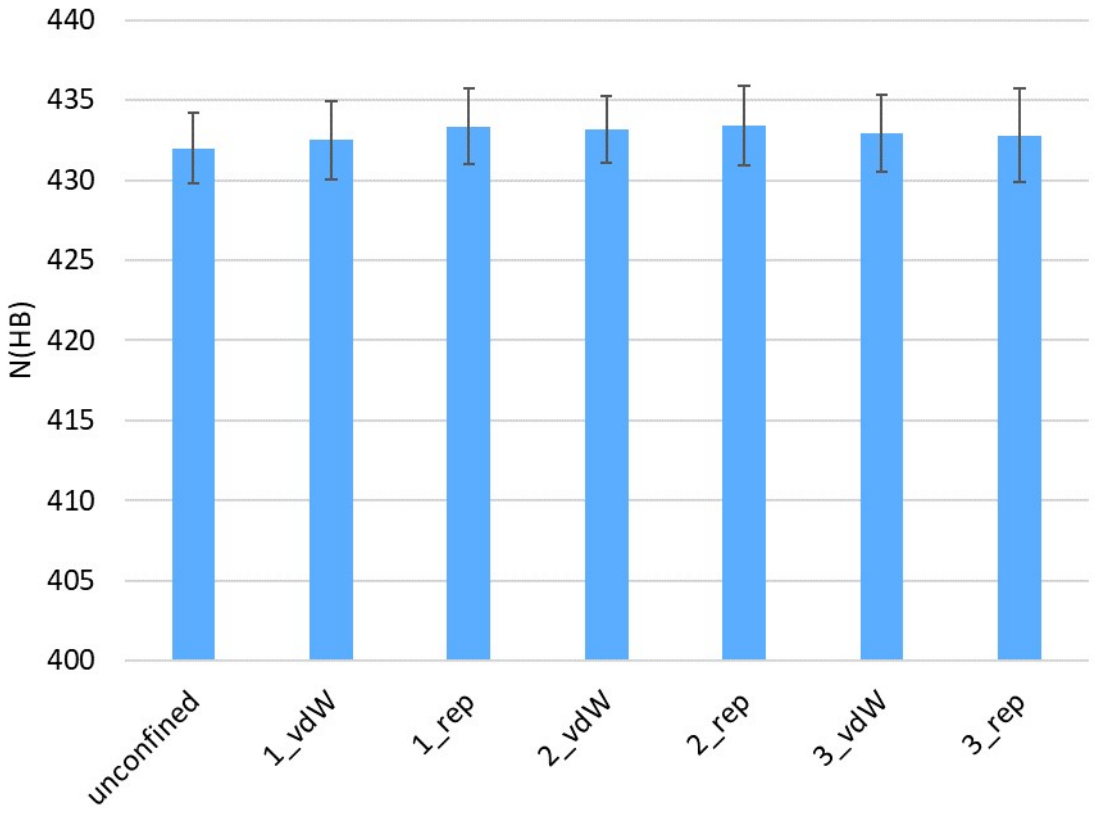

Figure S5. Average number of HBs per frame in the unconfined and confined liquids. The numbers 1, 2, 3 in the labels refer to nanolayer, nanotube and nanocavity respectively while vdW and rep stand for full van der Waals and repulsive-only potential to model the barriers. The average is performed over the last 200 frames (100 ps). The simulation box has 432 molecules.

S7. Local number density

Another feature of the structure of confined liquids is the inhomogeneous density of the system. BZA molecules tend to adsorb to the barriers, showing a higher density with respect to the bulk region (see text). Figure S6 describes how the liquid is structured in terms of average local number density, $<\rho_{loc}>$, in the nanocavity with full van der Waals and repulsive-only barriers. This quantity was evaluated by counting the number of molecular centers of mass within 0.1 Å-thick parallel slices between opposite pairs of van der Waals walls. The results were averaged over the three directions and over 600 frames (300 ps). The local density follows the expected trend. Very close to the walls $<\rho_{loc}> = 0$, as net repulsive forces prevail. At ~3 Å there is the main peak corresponding to the first layers of molecules adsorbed to the barriers while at larger *R*'s, the function shows a damped oscillatory trend with period of ~5 Å, roughly corresponding to the maximum molecular length along dipole axis, *i.e.* parallel to the Ph–COOH C1-C12 bond (Figure 1). This behavior is ascribable to the tendency of BZA to partially order in layers parallel to the barriers. Noteworthy, the same trend was observed in confined liquids made of rigid van der Waals spheres.[12]

As expected, the peak relative to the first layers of molecules interacting with the barriers with full van der Waals potential is shifted at lower distances. Both curves show a damped oscillatory behavior but have a different phase.

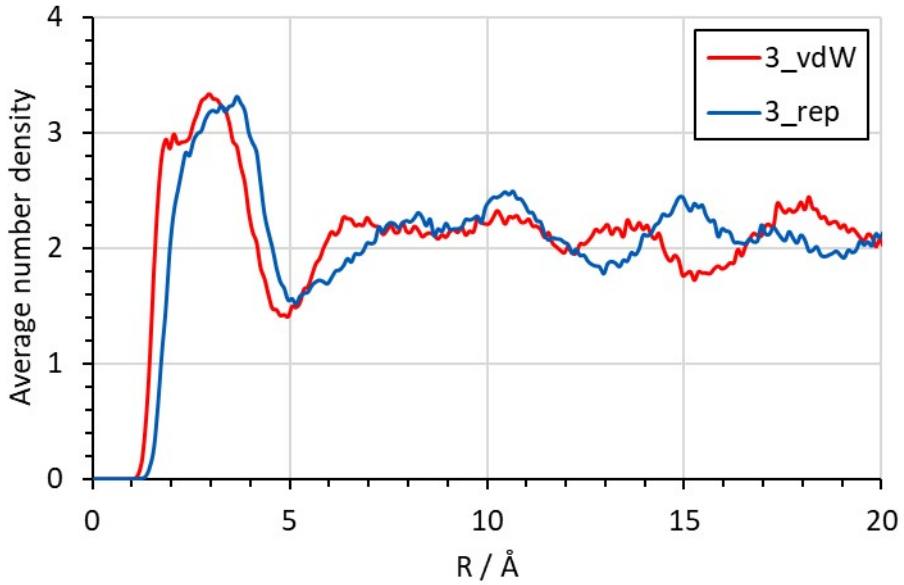

Figure S6. Local number density of molecular centers of mass as a function of the absolute distance from the barriers in the nanocavity with repulsive-only (blue) compared to full van der Waals (red) potential. The curves come from the average over the last 600 frames (300 ps) of the trajectory and over the three directions x, y, and z.

S8. Molecular orientations

Figure S7 reports the probability density distribution of molecule vectors $\mathbf{v}_1$ (Figure S7a) and $\mathbf{v}_2$ (Figure S7b) and the difference with respect to a random probability density distribution for the full van der Waals nanocavity simulation. Each point comes from the space average of all the molecules with centers of mass within 10 Å from each other, and from the corresponding time average over 600 frames (300 ps).

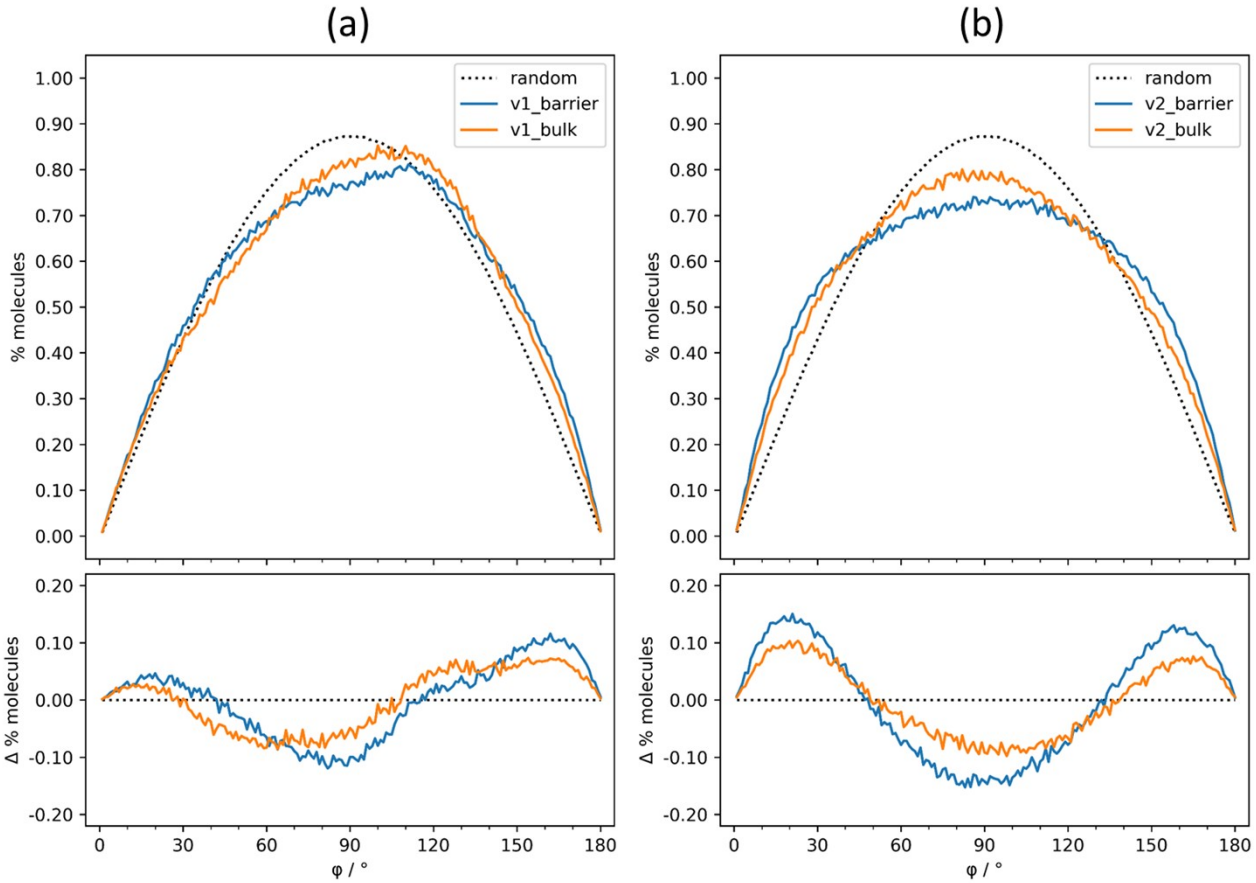

Figure S7. Top: probability density distribution of the angle between (a) vector $\mathbf{v}_1$ or (b) vector $\mathbf{v}_2$ of a reference molecule with respect to the same vector of adjacent molecules (with c.o.m. within 10 Å), expressed in % of molecules, for the nanocavity simulation with full van der Waals barriers. Bottom: differences with respect to a completely random distribution. Different curves are reported for molecules close to the barrier (<6.4 Å, full blue) and in the bulk (>6.4 Å, full orange) and a random distribution is also shown for comparison (dotted black). The results are averaged over the last 600 frames (300 ps) and over the three directions.

Figure S8 shows the probability density distribution of molecule vectors $\mathbf{v}_1$ (Figure S8a) and $\mathbf{v}_2$ (Figure S8b), with respect to the barrier normal vectors pointing inward within the simulation box. The average is carried out over the last 600 frames (300 ps).

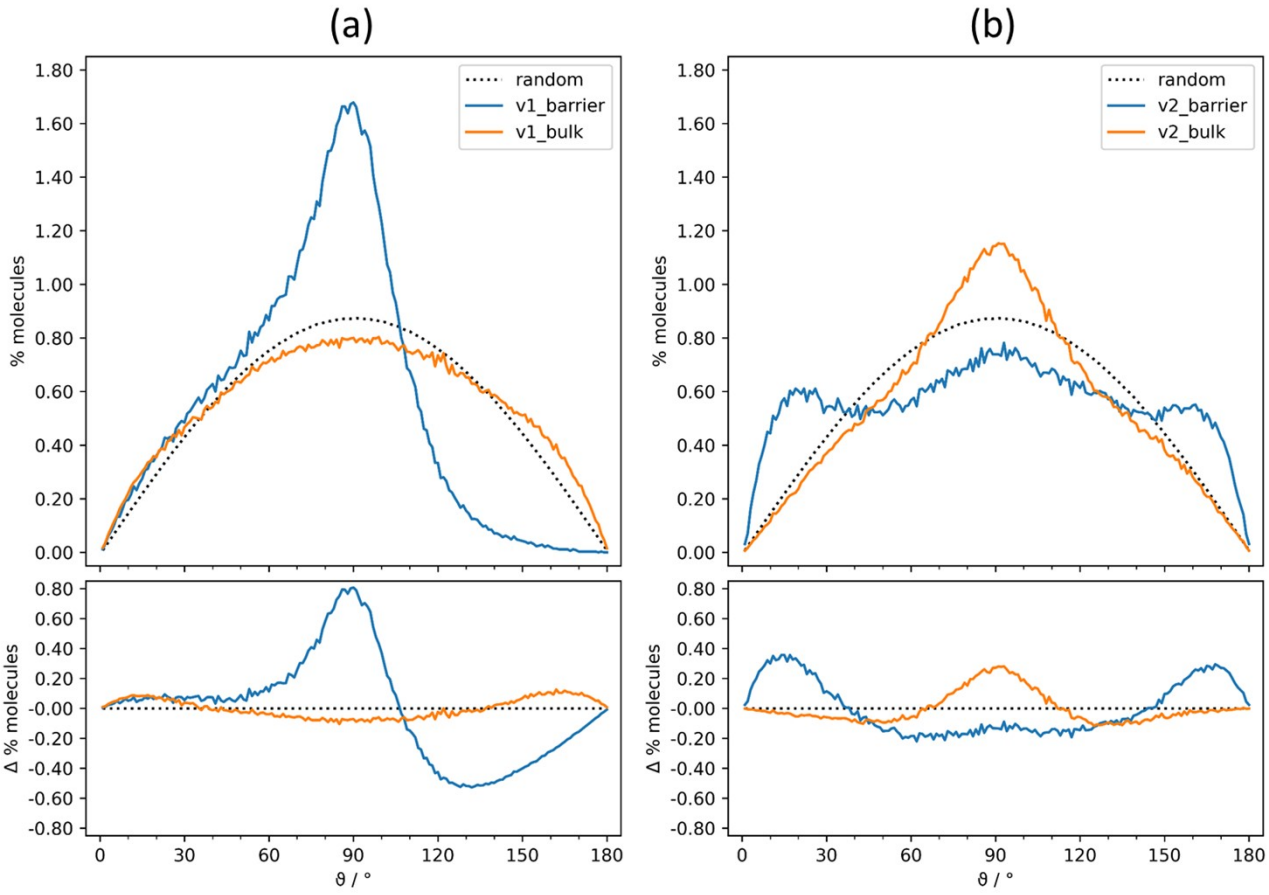

Figure S8. Top: probability density distribution of the angle between (a) vector $\mathbf{v}_1$ or (b) vector $\mathbf{v}_2$ and the barrier normal vectors pointing inward within the simulation box, expressed in % of molecules, for the nanocavity simulation with full van der Waals barriers. Bottom: differences with respect to a completely random distribution. Different curves are reported for molecules close to the barrier (d < 6.4 Å, full blue) and in the bulk (d > 6.4 Å, full orange) and a random distribution is also shown for comparison (dotted black). The results are averaged over the last 600 frames (300 ps) and over the three directions.

S9. Stiff barriers and liquid-liquid transitions

Table S6 reports the self-diffusion coefficients, viscosities and densities of nanolayer simulations with isotropic or anisotropic scaling, using barriers with stiff parallel constants ($s_{\parallel} = 0.050$). With full van der Waals barriers, the difference of viscosity is minimal while it is significant when repulsive-only potential is used.

Figure S9 shows the OH···O radial distribution function for the nanocavity simulation with full van der Waals barriers and isotropic stiff constants (s = 0.050), before and after the transition from high density (HD) to low density (LD). The HD state is characterized by a main peak that is more intense and shifted at lower distances with respect to the LD state. The same two states are found in the simulation with repulsive-only barriers as well.

Table S6. Effect of anisotropic scaling on self-diffusion coefficients (D), dynamic shear diffusion viscosities η and densities in confined nanolayers with stiff barriers. Standard deviations are reported in parentheses. The scaling factors of force constant orthogonal and parallel to the barriers are indicated as $s_{\perp}$ and $s_{\parallel}$.

$s_{\perp}$	$s_{\parallel}$	Barrier	$D \times 10^{-10}$ m^2·s^{-1}	$\eta \times 10^3$ Pa·s	ρ / g·cm^{-3}
0.010	0.050	Full vdW	1.352(6)	6.34(3)	1.150(7)
0.050	0.050	Full vdW	1.481(6)	5.79(3)	1.171(9)
0.010	0.050	Rep only	0.712(5)	12.05(9)	1.136(7)
0.050	0.050	Rep only	1.225(9)	7.00(6)	1.141(9)

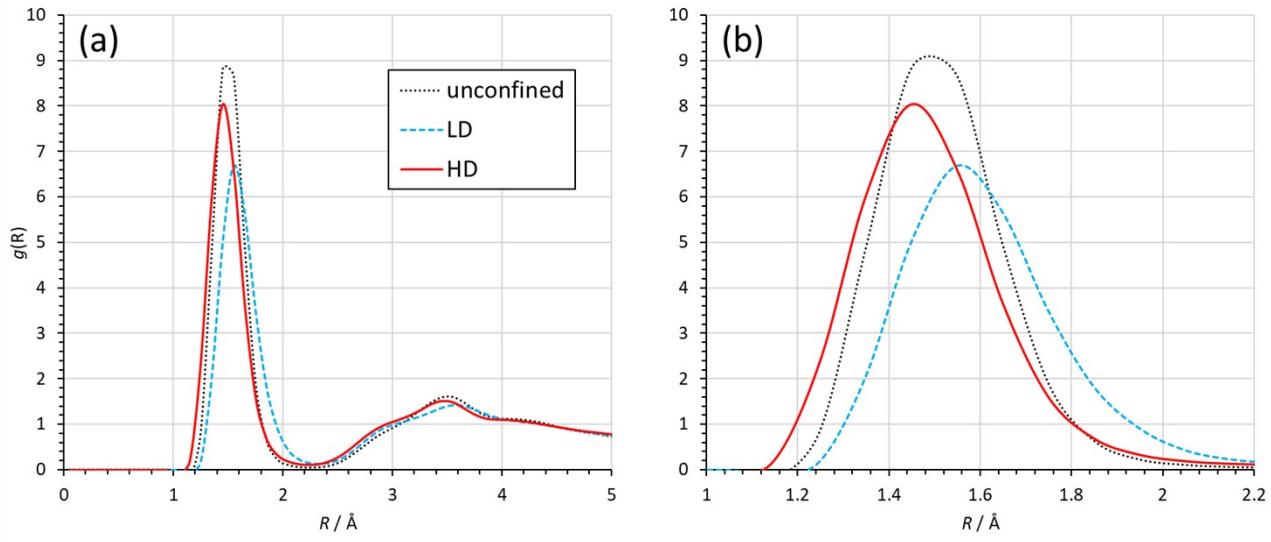

Figure S9. (a) Radial distribution functions (RDF) for the OH···O contacts in the HD (full red) and LD (dashed blue) states in the nanocavity with full van der Waals barriers, compared with the unconfined liquid (dotted black). Each curve comes from the average over 200 frames (100 ps) of the trajectory on each side of t_{onset}. (b) Detail of the main peak in the 1.0-2.2 Å region.

Figure S10 and Figure S11 show the liquid-liquid transitions observed in the nanocavity simulations with stiff barriers (scaling factor s = 0.05). Density and energies of 3 trajectories with full van der Waals barriers (Figure S10) and 3 trajectories with repulsive-only barriers (Figure S11), starting from an identical input. In all the 6 simulations, we detected more or less evident transitions, from high density to low density or vice versa. In these simulations, the local equilibrium approximation is no longer valid, and the microscopic behavior is determined by fluctuations at the nanoscale. This implies that the induction time for the liquid-liquid transition and its reversal is not deterministic. However, the outcomes are robust against fluctuations affecting individual trajectories.

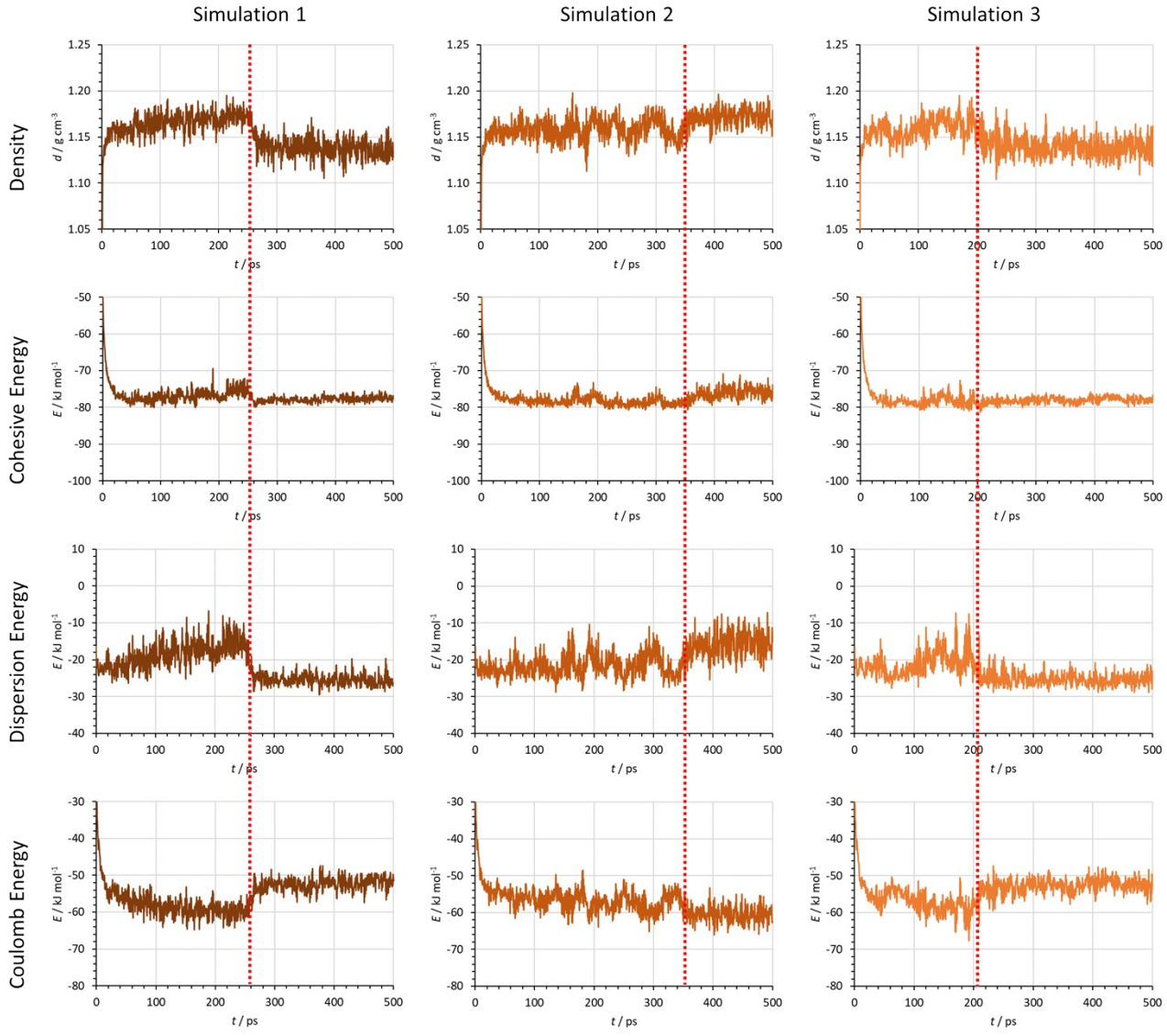

Figure S10. Density, cohesive energy, dispersion energy, and Coulomb energy (rows) for each of the 3 nanocavity simulations with barriers modeled by full van der Waals potential (columns). The dashed red vertical lines highlight the time at which the transitions take place.

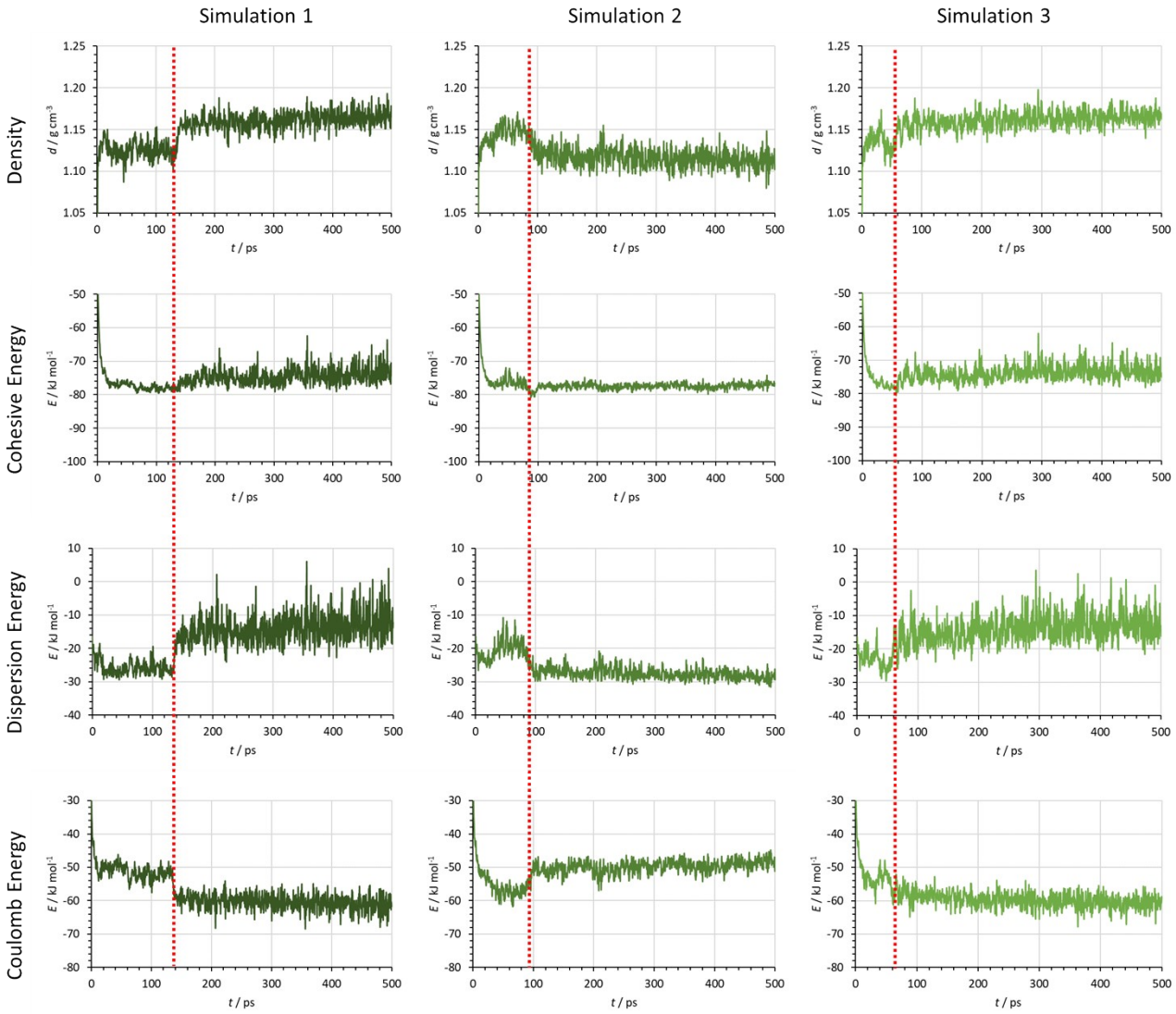

Figure S11. Density, cohesive energy, dispersion energy, and Coulomb energy (rows) for each of the 3 nanocavity simulations with barriers modeled by repulsive-only potential (columns). The dashed red vertical lines highlight the time at which the transitions take place.

Figure S12 shows the time evolution of monomers, cyclic dimers and cyclic trimers in the nanocavity simulation with repulsive-only barriers. In the low density state (t < 134 ps), the quantity of cyclic trimers in the barrier region is lower compared to the corresponding value for the high-density state.

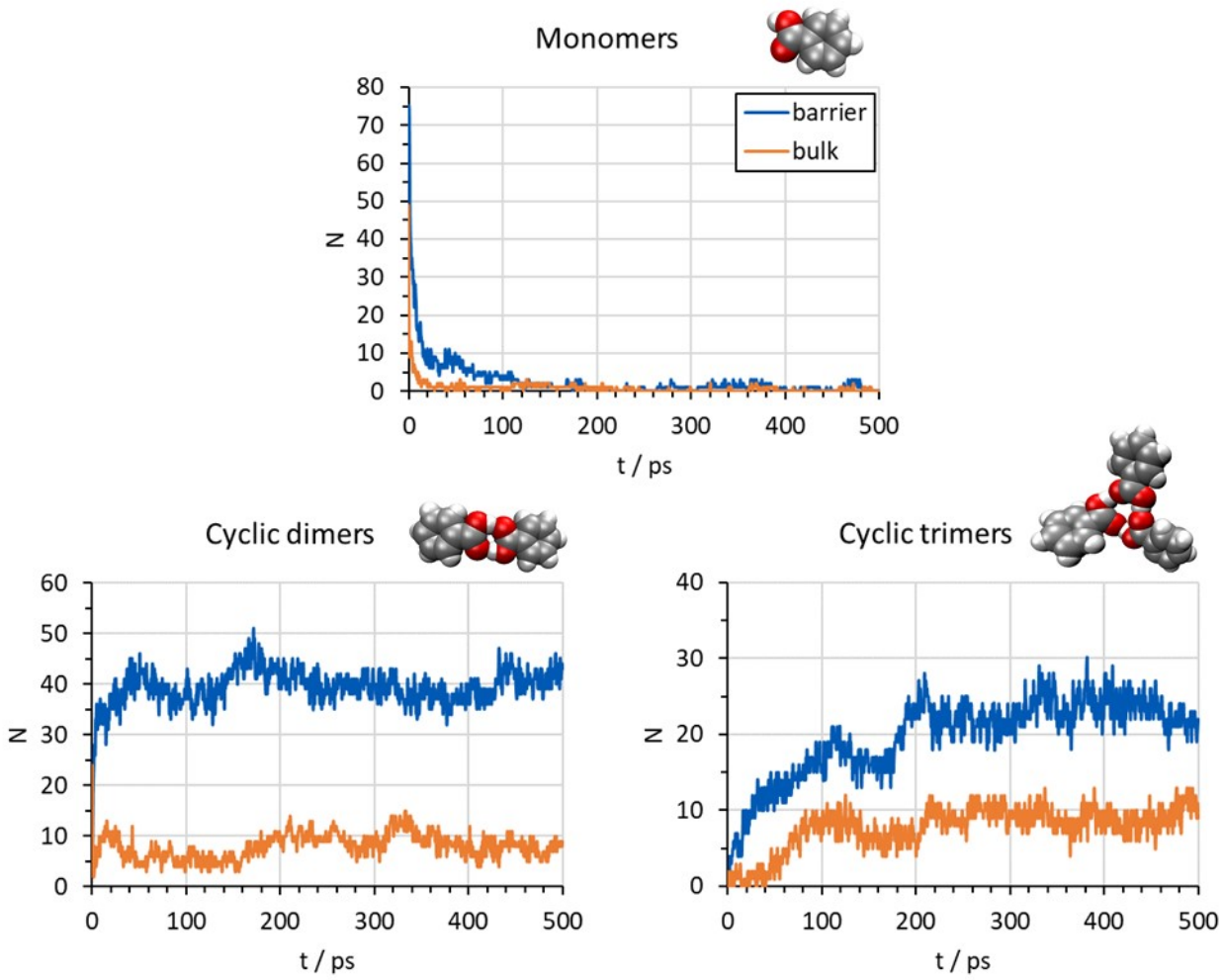

Figure S12. Time evolution of the number of monomers, cyclic dimers and cyclic trimers in the nanocavity simulation with repulsive-only barriers. The graph distinguishes between two different regions: barrier (blue) and bulk (orange), as depicted in Figure 2 of the main text. Aggregates are considered in the barrier region if the distance of all the centers of mass from the barriers is below 10 Å.

Figure S13 shows the density distribution of molecule vectors $\mathbf{v}_1$ with the surrounding molecules, in the barrier and bulk region (Figure S13a,b), and with the barriers (Figure S13c,d) in the nanocavity simulation with repulsive-only barriers. Differently from Figure S7 and Figure S8, the molecular orientations are shown in terms of average number instead of percentage of molecules, in order to better highlight the absolute differences.

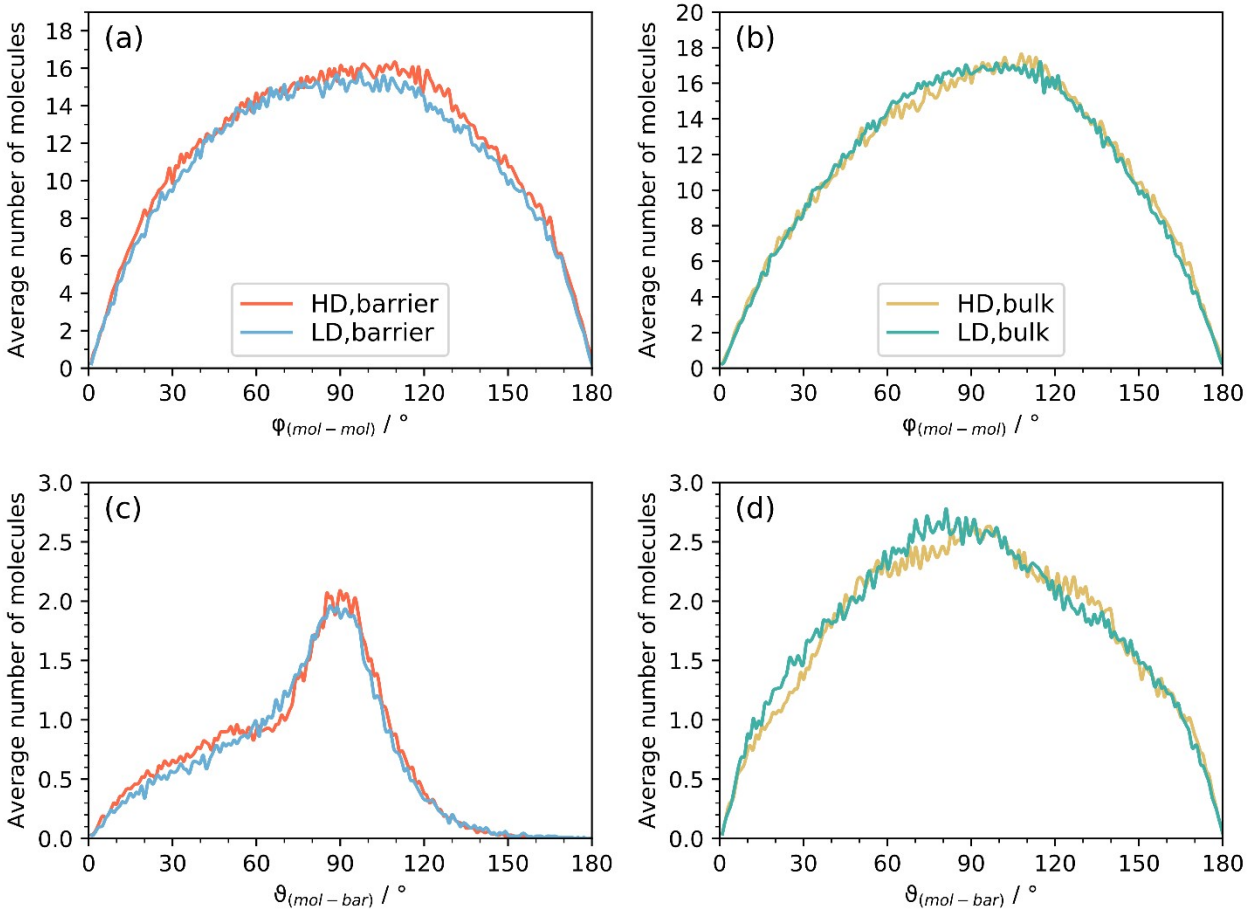

Figure S13. (a) Density distribution of molecule vectors $\mathbf{v}_1$ with the other molecules in the barrier region. (b) Same, in the bulk region. (c) Density distribution of molecule vectors $\mathbf{v}_1$ with the vectors orthogonal to the barriers, pointing inward, in the barrier region. (d) Same, in the bulk region. Data comes from the nanocavity simulation with repulsive-only barriers. The results are averaged over 200 frames (100 ps) before or after the transition and over the three directions.

References

1 L. Lo Presti, S. Rizzato, G. Macetti and L. Sironi, MiCMoS Users' Manual - MIlano Chemistry MOlecular Simulation v2.1, 2022, 1–158.

2 A. Zaccone, Explicit Analytical Solution for Random Close Packing in d=2 and d=3, *Phys Rev Lett*, 2022, **128**, 028002.

3 A. Gavezzotti and L. Lo Presti, Dynamic simulation of liquid molecular nanoclusters: structure, stability and quantification of internal (pseudo)symmetries, *New Journal of Chemistry*, 2019, **43**, 2077–2084.

4 M. Stroet, B. Caron, K. M. Visscher, D. P. Geerke, A. K. Malde and A. E. Mark, Automated Topology Builder Version 3.0: Prediction of Solvation Free Enthalpies in Water and Hexane, *J Chem Theory Comput*, 2018, **14**, 5834–5845.

5 D. Van Der Spoel, E. Lindahl, B. Hess, G. Groenhof, A. E. Mark and H. J. C. Berendsen, GROMACS: Fast, flexible, and free, *J Comput Chem*, 2005, **26**, 1701–1718.

6 H. J. C. Berendsen, J. P. M. Postma, W. F. van Gunsteren, A. DiNola and J. R. Haak, Molecular dynamics with coupling to an external bath, *J Chem Phys*, 1984, **81**, 3684–3690.

7 G. Bussi, D. Donadio and M. Parrinello, Canonical sampling through velocity rescaling, *Journal of Chemical Physics*, 2007, **126**, 014101.

8 B. Hess, H. Bekker, H. J. C. Berendsen and J. G. E. M. Fraaije, LINCS: A linear constraint solver for molecular simulations, *J Comput Chem*, 1997, **18**, 1463–1472.

9 T. Darden, D. York and L. Pedersen, Particle mesh Ewald: An N·log(N) method for Ewald sums in large systems, *J Chem Phys*, 1998, **98**, 10089.

10 R. Kohlrausch, Ueber das Dellmann'sche Elektrometer, *Annalen der Physik und Chemie*, 1847, **148**, 353–405.

11 W. Graham and D. C. Watts, Non-Symmetrical Dielectric Relaxation Behaviour Arising from a Simple Empirical Decay Function, *Transaction of the Faraday Society*, 1970, **66**, 80–85.

12 S. Granick, Motions and Relaxations of Confined Liquids, *Science*, 1991, **253**, 1374–1379.